International Journal of Engineering, Mathematical and Physical Sciences
ISSN: 2517-9934
Vol:6, No:5, 2012

Dynamics and Control of a Chaotic Electromagnetic System

Shun-Chang Chang

***Abstract*—**In this paper, different nonlinear dynamics analysis techniques are employed to unveil the rich nonlinear phenomena of the electromagnetic system. In particular, bifurcation diagrams, time responses, phase portraits, Poincare maps, power spectrum analysis, and the construction of basins of attraction are all powerful and effective tools for nonlinear dynamics problems. We also employ the method of Lyapunov exponents to show the occurrence of chaotic motion and to verify those numerical simulation results. Finally, two cases of a chaotic electromagnetic system being effectively controlled by a reference signal or being synchronized to another nonlinear electromagnetic system are presented.

***Keywords*—**bifurcation, Poincare map, Lyapunov exponent, chaotic motion.

I. Introduction

IT is well known that the characteristics of magnetic bearings are inherently nonlinear due to the nonlinearities of electromagnetic forces. To accurately control or predict the performance of this system, the effects of these nonlinearities must be taken into consideration. Therefore, in our previous work [1], an experiment with a symmetric rotor with a spring device, as shown in Figure 1, was carried out by applying a series of nonlinear electromagnetic forces to identify a nonlinear model for the system.

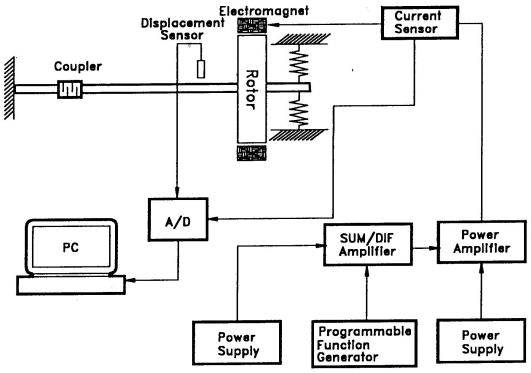

Fig. 1 Schematic diagram of the electromagnetic system

For easy reference, the experimental results are presented in the previous work [1]. These experimental results show the frequency responses of the rotor displacement for an input amplitude 3.0 V in decreasing forcing frequency (ω) from 80 Hz to 34.4 Hz. It can be seen that if the system starts at high frequency and the forcing frequency is slowly decreased, there is an increase in amplitude along the resonant part of the response curve.

S. C. Chang is with the Department of Mechanical and Automation Engineering, Da-Yeh University, Changhua 51591, Taiwan, R.O.C.(e-mail: changsc@ mail.dyu.edu.tw).

The smooth variations in amplitude and frequency continue until ω = 37.6 Hz, where the first period-doubling bifurcation occurs. In this type of period-doubling bifurcation a stable limit cycle loses its stability, while another closed orbit is born whose period is twice the period of the original oscillation. Beyond this point, the vibrating amplitude of the rotor and the coil current grow sharply. As the forcing frequency continues to decrease, the trajectory continues to experience period-doubling bifurcations, which eventually result in likely chaotic motion, and finally the rotor strikes the electromagnet, i.e., the system blows up. This shows that the system exhibits complicated nonlinear behavior due to the nonlinearities of the electromagnetic force. In engineering applications, this should be taken into consideration at the design stage.

To study the dynamics of this system further we have modified the conventional identification technique based on the principle of harmonic balance to identify this system. The resulting nonlinear model [1] is obtained as:

$$\frac{d^2y}{dt^2} + b_1\frac{dy}{dt} + b_2 y + b_3 y^2 + b_4 y^3 + b_5(I_0+i)^{6/3} + b_6(I_0+i)^{2/3} + b_7(I_0+i)^{4/3} + b_0 = 0 \quad \text{(1a)}$$

$$L_1(I_0+i)^{-1}\frac{di}{dt} + iR = K_A A_0 \sin(\omega t), \quad \text{(1b)}$$

where I_0 is the biased current calculated directly from the average experimental current time series, i is the oscillating current about I_0 (= 0.68 Amp), y is the oscillating displacement of the rotor about a reference point, R is the resistance of the coil, and K_A (= 2.254) is the power amplifier gain. The other necessary coefficients for (1) are listed in Table I.

TABLE I
Identified Results

Identified value	System parameter
43.84	b_1
1.75×10^4	b_2
3.97×10^4	b_3
-16.81×10^4	b_4
3.31×10^4	b_5
10.51×10^4	b_6
-9.98×10^4	b_7
-3.44×10^4	b_0
0.018	L_1
9.79	R

This model successfully captures the primary characteristics of the system by comparing the frequency responses from simulations to those from experiments. However, theoretical analyses of this model showing whether the identified nonlinear mathematical model obtained from the experiment can predict and characterize the dynamics of the real system have not yet been carried out.

Furthermore, the occurrence of chaotic motion at the moment the rotor strikes the electromagnet has also not been undertaken.

In this paper, many numerical simulation methods have been employed to study the dynamical behavior of the system, such as, bifurcation diagrams, time responses, Poincare maps, power spectrum analysis. The method of Lyapunov exponents [2] is also applied to show the occurrence of chaotic motion.

In many engineering problems of chaos control it is important to develop control techniques to drive a chaotic attractor to a periodic orbit. Since the pioneering work of Ott, Grebogi and Yorke [3] in controlling chaos, many modified methods and other approaches have successively been proposed [4-9]. As for the synchronization of chaos, many efforts have been made, for example, the works studied by [10-14]. Usually, one chaotic system is referred to as the master (drive) system and the other as the slave (response) system. The basic idea of synchronization is to use the output of the master system to control the slave system so that the output of the slave system follows the output of the master system asymptotically. Some attempts to solve the problem have been made recently [13-15]. Finally, in this paper, in order to improve the performance of a dynamics system or avoid the chaotic behavior, sometimes we have to convert a chaotic behavior into a periodic motion. Two methods are presented to control and suppress chaos: synchronization by a sinusoidal signal and synchronization by another nonlinear electromagnetic system [13].

II. Bifurcation Diagrams And Lyapunov Exponents

The equations of motion were nondimensionalized in order to transform the system into the dimensionless domain, in which the behavior of different physical systems can conveniently be compared. The time t was nondimensionalized by using the electromagnetic system natural frequency (ω_n). For convenience, we first let $\omega_n = \sqrt{b_2}$, $\Omega = \omega / \omega_n$, $\tau = \omega_n t$, $x_1 = y$, $x_2 = y'$ and $x_3 = i$, and normalize (1) to a set of ordinary differential equations:

$$x_1' = x_2 \tag{2a}$$

$$x_2' = f(x_1, x_2, x_3) \tag{2b}$$

$$x_3' = \frac{(K_A A_0 \sin(\Omega\tau) - x_3 R)(I_0 + x_3)}{L_1 \omega_n} \tag{2c}$$

$$f(x_1, x_2, x_3) = -x_1 - (\frac{b_1}{\omega_n})x_2 -$$

where, $\frac{(b_3 x_1^{\,2} + b_4 x_1^{\,3} + b_5 (I_0 + x_3)^{6/3} + b_6 (I_0 + x_3)^{2/3})}{\omega_n} -$

$$\frac{(b_7 (I_0 + x_3)^{4/3} + b_0)}{\omega_n} .$$

To clearly understand the characteristics of this system, we carry out a series of numerical simulations from (2). The commercial package DIVPRK of IMSL in FORTRAN subroutines for mathematics applications is used to solve ordinary differential equations [16]. The resulting bifurcation diagram is shown in Fig. 2. It can be clearly seen from this figure that the first period-doubling bifurcation occurs at about $\Omega = 1.863$, and that at $\Omega = 1.715$ chaotic motion appears. More details about the various responses exhibited by the system are presented in Figures 3. There, each type of response is characterized by a Poincare map (Poincare velocity vs. phase angle) and frequency spectrum. Fig. 3(a) and 3(b) show that the T_f -period mainly involves the constant term and the fundamental components. From Fig. 3(c) to 3(d), we find that a cascade of period-doubling bifurcations causes a series of subharmonic components, which show the bifurcations with new frequency components at $\Omega/2$, $3\Omega/2$, $5\Omega/2$, …. The particular features of two descriptors characterize the essence of the chaotic behavior: the Poincare map and the frequency spectrum. The Poincare map shows an infinite set of points referred to as a "strange attractor." Simultaneously, the frequency spectrum of chaotic motion is a continuous broad spectrum. The two features – "strange attractor" and continuous type Fourier spectrum – are strong indictors of chaos. Chaotic motions are shown in Fig. 3(g) and 3(h).

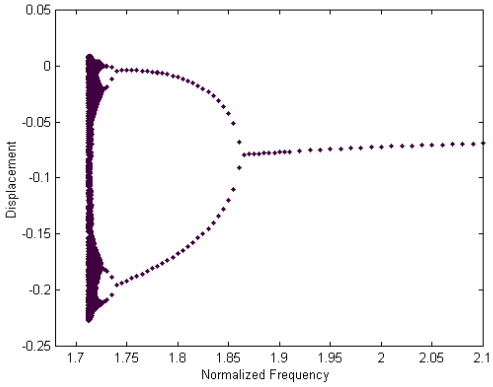

Fig. 2 Bifurcation diagram of the system for $A_0 = 3.0$ V.

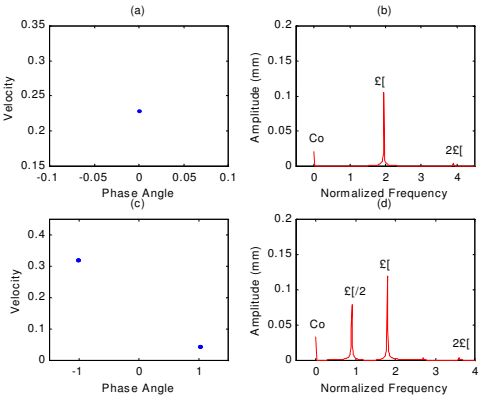

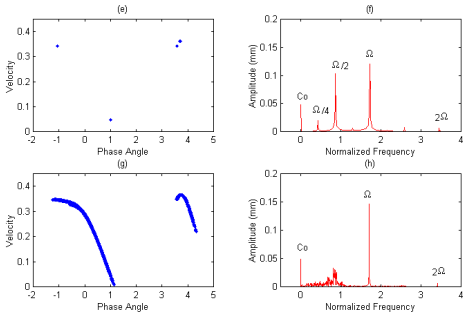

Fig. 3 Frequency spectra and Poincare maps of various responses of numerical simulations for A_0 = 3.0 V:
(a) and (b) period-one motion, Ω = 1.95;
(c) and (d) period-two motion, Ω = 1.80;
(e) and (f) period-four motion, Ω = 1.7255;
(g) and (h) chaotic motion, Ω = 1.708.

The occurrence of chaotic motion can be verified by means of Lyapunov exponents analysis. For every dynamic system, there is a spectrum of Lyapunov exponents (λ) [2] that tell how length, areas and volumes change in phase space. As a criterion for the existence of chaos, one needs only to calculate the largest exponent, which tells whether nearby trajectories diverge ($\lambda > 0$) or converge ($\lambda < 0$) on average. Any bounded motion in a system containing at least one positive Lyapunov exponent is defined as chaotic, while for periodic motion, the Lyapunov exponents are not positive. Referring to the algorithm for calculating the Lyapunov exponents described by Wolf *et al.* [2], the evolution of the largest Lyapunov exponent for $A_0 = 3.0$ V is computed as displayed in Figure 4. From this figure, we find that the onset of chaotic motion is at Ω =1.710, because at this point, P_4, the largest Lyapunov exponent, changes its sign from negative to positive when the normalized forcing frequency is slowly decreased. For points $P_{1\text{-}3}$, the largest Lyapunov exponents are shown to approach zero. The system at these points may undergo bifurcations. However, the Lyapunov exponent at such a point provides no means to determine the type of bifurcation, so that the bifurcation diagram presented in Fig. (2) must be applied. For example, in Fig.(2), the occurrence of the first period-doubling bifurcation at about Ω =1.860, while point P_1, where the largest Lyapunov exponent first approaches zero, is found at Ω =1.8475.

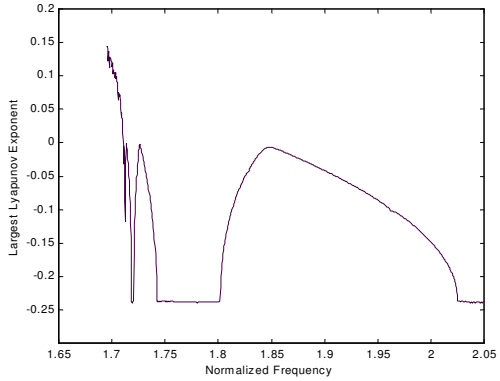

Fig. 4 The largest Lyapunov exponents of the system for A_0 = 3.0 V.

When the forcing frequency is larger than P_1, $\Omega = 1.95$; as an example, the Lyapunov exponents computed from (2) are λ_1 = –0.082501, λ_2 = –0.396172, and λ_3 = –4.017426. Their sum is $\lambda_1+\lambda_2+\lambda_3$ = -4.496099, which is negative, showing that the motion of the rotor at these values finally converges to a stable limit cycle. Indicating with $\lambda_1 \geq \ldots \geq \lambda_n$ the Lyapunov exponents of a dynamical system, Kaplan and Yorke [17] provide an estimation for the Lyapunov dimension d_L as:

$$d_L = j + \frac{1}{|\lambda_{j+1}|}\sum_{i=1}^{j}\lambda_i \,, \qquad (3)$$

where j is the largest integer that satisfies $\sum_{i=1}^{j}\lambda_i > 0$. By applying the technique, the Lyapunov dimension of (2) for $\Omega = 1.95$ is d_L =1. Because the value of the Lyapunov dimension is an integer, the system has a periodic motion. When the forcing frequency Ω decreases across the bifurcation point, for example Ω =1.708, the Lyapunov exponents are $\lambda_1 = 0.1447$, $\lambda_2 = -0.6234$ and $\lambda_3 = -4.01773$. Here, the Lyapunov dimension is d_L=2.232. It should be noted that the value of the Lyapunov dimension is not an integer; the system at this point can process fractal basin boundaries [18]. This reveals that a measure of the fractal geometry of the attractor and the property of sensitivity dependence on initial conditions exist in the system. Fig. 5 shows the fractal basin boundaries in such a case, with fixed $A_0 = 3.0$ V, $\Omega = 1.708$ and various initial conditions. For calculation [19], 1600 × 250 sets of initial conditions were chosen in the form of a grid, and integration of (2) using a fifth-order Runge-Kutta integration algorithm was continued until the system either converged to the bounded attractors or diverged. Initial conditions in the light regions lead to the divergent solutions, while the dark regions are the basins for the bounded attractors. The fractal structure points out that small uncertainties in the initial conditions can lead to unpredictability of the system output.

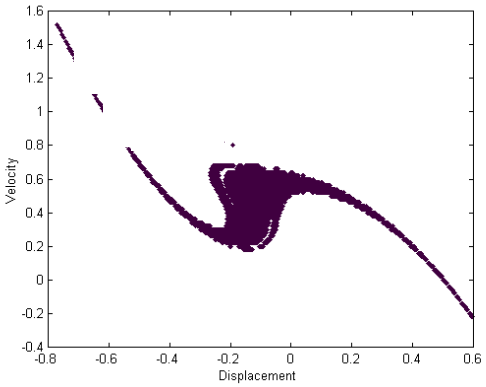

Fig. 5 Fractal basin boundaries of the system for A_0 = 3.0 V at Ω = 1.708

III. Synchronization And Control Of Chaos

From the Lyapunov exponents and the bifurcation diagram, we can clearly find that the chaotic motion is seen to occur at about $\Omega \le 1.710$. Now, the chaotic system considered in this paper is given as follows:

$$x_1' = x_2 \tag{4a}$$
$$x_2' = f(x_1, x_2, x_3) + u(\tau) \tag{4b}$$
$$x_3' = \frac{(K_A A_0 \sin(\Omega\tau) - x_3 R)(I_0 + x_3)}{L_1 \omega_n}, \tag{4c}$$

where $f(x_1, x_2, x_3)$ is a nonlinear function and $u(\tau)$ is the control signal that is to be designed. The main goal of the control is to determine $u(\tau)$ based on $y(\tau)$ that is an arbitrarily given reference signal and its derivatives so that:

$$\left|x_1(\tau) - y(\tau)\right| \to 0, \quad \text{as } \tau \to \infty \tag{5}$$

Let α_1 and α_2 be any two positive constants and defined:

$$u(\tau) = -f(x_1, x_2, x_3) - \alpha_1 x_1 - \alpha_2 x_2 + (y'' + \alpha_2 y' + \alpha_1 y) \tag{6}$$

Substitute (6) into (4) and obtain:

$$x_1' = x_2 \tag{7a}$$
$$x_2' = -\alpha_1 x_1 - \alpha_2 x_2 + (y'' + \alpha_2 y' + \alpha_1 y) \tag{7b}$$
$$x_3' = \frac{(K_A A_0 \sin(\Omega\tau) - x_3 R)(I_0 + x_3)}{L_1 \omega_n}, \tag{7c}$$

where α_1 and α_2 are the constant feedback gains.

In the following, a chaotic system is controlled by a reference signal or is synchronized to another nonlinear system are discussed [13].

A. Synchronization by a sinusoidal signal

We consider the chaotic system for (3) at $\Omega = 1.708$. We adopt the control signal, $u(\tau)$, (such as (6)) and plot the stability region in the α_1 and α_2 plane, as shown in Fig. 6. So, if the chaos will be controlled to the period motion, then the choice of α_1 and α_2 should be taken from stability region. On the other hand, the feedback gains α_1 and α_2 should be two positive constants except from empty region in Fig.(6). After a time $\tau = 150$, as the values $\alpha_1 = 1$ and $\alpha_2 = 1$, the chaotic electromagnetic system is to be synchronized with the sinusoidal signal,

$$y(\tau) = 0.2\sin(0.2\tau). \tag{8}$$

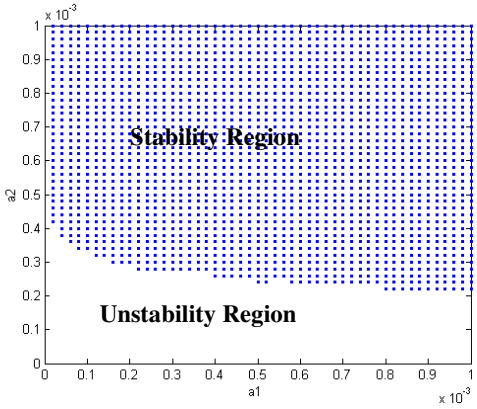

Fig. 6 The stability and unstability regions of the controlled system with sinusoidal signal.

The synchronization errors, $\varepsilon_1(\tau) = x_1(\tau) - y(\tau)$ and $\varepsilon_2(\tau) = x_2(\tau) - y'(\tau)$, are shown in Fig. (7), respectively. The time response of x_1 is shown in Fig. (8a) where the control signal is added after $\tau = 150$. The chaotic system is controlled with the sinusoidal signal and converges into a period motion. The phase portrait of the controlled system is shown in Fig. (8b).

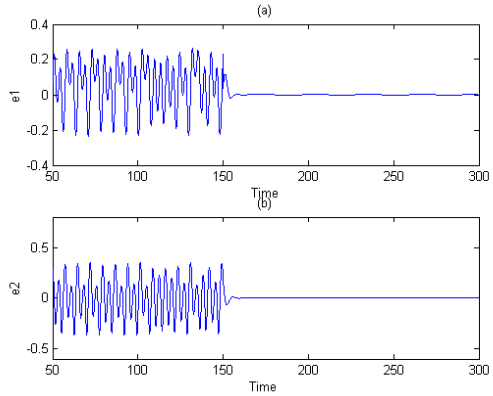

Fig. 7 The synchronization errors via the controlled system with the sinusoidal signal

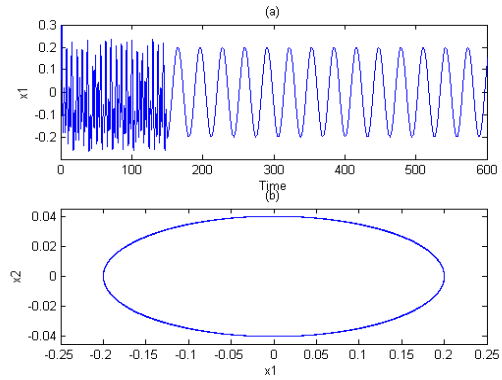

Fig. 8 Injecting a sinusoidal signal control which is used to control chaotic motion of the system for $A_0 = 3.0$ V at $\Omega = 1.708$. The sinusoidal signal is added after a time $\tau = 150$:(a)time response; (b)controlled orbit.

B. Synchronization by another nonlinear electromagnetic system

We choose the slave electromagnetic system given by:

$$x_1' = x_2 \tag{9a}$$
$$x_2' = f(x_1, x_2, x_3) + u(\tau) \tag{9b}$$
$$x_3' = \frac{(K_A A_0 \sin(1.708\tau) - x_3 R)(I_0 + x_3)}{L_1 \omega_n}. \tag{9c}$$

The master electromagnetic system, where we have changed the forcing frequency in the slave system as follows:

$$y_1' = y_2 \tag{10a}$$
$$y_2' = f(y_1, y_2, y_3) \tag{10b}$$
$$y_3' = \frac{(K_A A_0 \sin(1.9\tau) - y_3 R)(I_0 + y_3)}{L_1 \omega_n}. \tag{10c}$$

According to (6), the control signal, $u(\tau)$, is provided by:

$$u(\tau) = -f(x_1, x_2, x_3) - \alpha_1 x_1 - \alpha_2 x_2 + (y_1'' + \alpha_2 y_1' + \alpha_1 y_1). \tag{11}$$

We adopt the control signal, $u(\tau)$, (such as (11)) and plot the stability region in the α_1 and α_2 plane, as shown in Fig. (9). So, if the chaos will be controlled to the period motion, then the choice of α_1 and α_2 should be taken from stability region. In other words, the feedback gains α_1 and α_2 should be two positive constants except from empty region in Fig. (9) After a time $\tau = 300$, the chaotic electromagnetic system is to be synchronized by the control signal when $\alpha_1 = 1$ and $\alpha_2 = 1$. The synchronization errors, $\varepsilon_1(\tau) = x_1(\tau) - y_1(\tau)$ and $\varepsilon_2(\tau) = x_2(\tau) - y_1'(\tau)$, are shown in Figs. (10), respectively.

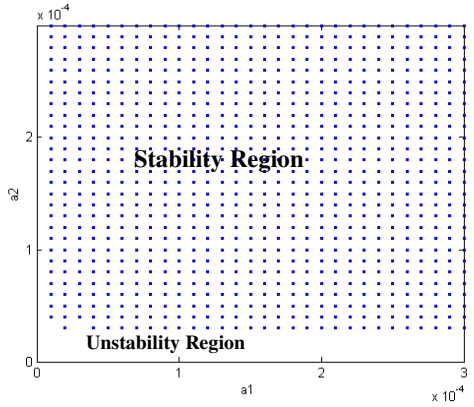

Fig. 9 The stability and unstability regions of the controlled system with a reference signal which generated by an electromagnetic system

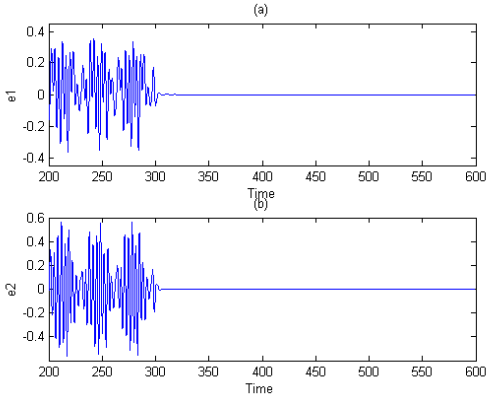

Fig. 10 The synchronization errors via the controlled system with a reference signal which generated by an electromagnetic system

The chaotic system is controlled with the sinusoidal signal and converges into a period motion. The control signal is added after $\tau = 300$, the time response of x_1 is shown in Fig. (11a) and the phase portrait of the controlled system is shown in Fig. (11b).

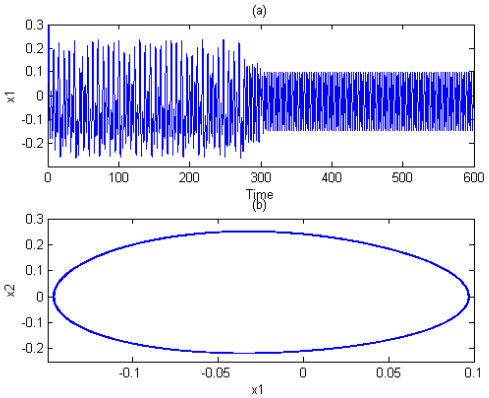

Fig. 11 Injecting a reference signal which generated by an electromagnetic system, which is used to control chaotic motion of the system for $A_0 = 3.0$ V at $\Omega = 1.708$. The controll signal is added after a time $\tau = 150$: (a)time response; (b)controlled orbit

IV. Conclusions

The nonlinear response characteristics of an electromagnetic system have been studied in order to unveil the nonlinear dynamic behavior, which has been displayed in bifurcation diagrams. In this paper, many numerical simulation methods have been employed to study the dynamical behavior of the system. An interpretation of the periodic and chaotic motion has been offered based on time responses, phase portraits, Poincare maps and power spectrum analysis. Furthermore, the chaotic motion has been detected by using Lyapunov exponents and Lyapunov dimensions effectively.

The presence of chaotic behavior is generic for certain nonlinearities, ranges of parameters and external force, where one wishes to avoid or control so as to improve the performance of a dynamic system.

Two cases of a chaotic electromagnetic system being successfully controlled by a reference signal or being synchronized to another electromagnetic system are presented. Thus, we can also efficiently suppress chaos and convert the chaotic system into a periodic orbit. Finally, the stability and unstability regions of the controlled system in control parameters space, α_1 and α_2, are found.

ACKNOWLEDGMENT

The author would like to thank the Department of Industrial Technology, Ministry of Economic Affairs, Taiwan, for financially supporting this research under Contract No. 100-EC-17-A-16-S1-127-C1. And it was also supported by the National Science Council in Taiwan, Republic of China, under project number NSC 100-2221-E-212 -019 -.

REFERENCES

[1] S. C. Chang, T. C. Tung, "Identification of a non-linear electromagnetic system: an experimental study," Journal of Sound and Vibration, vol. 214, pp. 853-872, 1998.
[2] A. Wolf, J. B. Swift, H. Swinney and J. A. Vastano, "Determining Lyapunov exponents from a time series," Physica D, vol. 16, pp. 285-317, 1985.
[3] E. Ott, C. Grebogi and J. A. Yorke, "Controlling chaos," Physical Review Letters, vol. 64, pp. 1196-1199, 1990.
[4] W. L. Ditto, S. N. Rauseo and M. L. Spano, "Experimental control of chaos," Physical Review Letters, vol. 65, pp. 3211-3214, 1990.
[5] E. R. Hunt, "Stabilizing high-period orbits in a chaotic system: The diode resonator," Physical Review Letters, vol. 67, pp. 1953-1955, 1991.
[6] Y. C. Lai, M. Ding and C. Grebogi, "Controlling Hamiltonian chaos," Physical Review E, vol. 67, pp. 86-92, 1993.
[7] C. Cai, Z. Xu, W. Xu and B. Feng, "Notch filter feedback control in a class of chaotic systems," Automatica, vol. 38, pp. 695-701, 2002.
[8] C. Cai, Z. Xu and W. Xu, "Converting chaos into periodic motion by feedback control," Automatica, vol. 38, pp. 1927-1933, 2002.
[9] C. C. Fun, P. C. Tung, "Experimental and analytical study of dither signals in a class of chaotic system," Physics Letters A, vol. 229, pp. 228-234, 1997.
[10] L. M. Pecora and T. L. Carroll, "Synchronization in Chaotic Systems," Physical Review Letters, vol. 64, pp. 821-823, 1990.
[11] J. K. John and R. E. Amritkar, "Synchronization by feedback and adaptive control," International Journal of Bifurcation and Chaos, vol. 4, pp. 1687-1695, 1994.
[12] S. Li and Y. P. Tian, "Finite time synchronization of chaotic systems," Chaos, Solitons & Fractals, vol. 15, pp. 303-310, 2003.
[13] E. W. Bai and K. E. Lonngren, "Synchronization and Chaos of Chaotic Systems," Chaos, Solitons & Fractals, vol. 10, pp. 1571-1575, 1999.
[14] T. L. Carroll, L. M. Pecora, "Synchronizing Chaotic Circuits," IEEE Trans. Circ Syst. I, vol. 38, pp. 453-456, 1991.
[15] T. L. Liao and S. H. Tsai, "Adaptive Synchronization of Chaotic Suystem and its Application to Secure Communications," Chaos, Solitons & Fractals, vol. 11, pp. 1387-1396, 2000.
[16] IMSL, Inc, User's manual – IMSL MATH/LIBRARY, 1989, pp. 633.
[17] J. L. Kaplan, J. A. Yorke, Chaotic behavior of multidimensional difference equations, Lecture Notes in Mathematics. New York: Springer-Verlag, 1979, pp.228-237.
[18] W. Szemplinska-Stupnicka, G. Iooss and F. C. Moon, Chaotic Motions in Nonlinear Dynamical Systems. New York: Springer-Verlag, 1988.
[19] C. Y. Tseng, P. C. Tung, "Stability, bifurcation, and chaos of a structure with a non-linear actuator," Japanese Journal of Applied Physics, vol. 34, pp. 3766-3774, 1995.